A Novel Method for Drug Delivery: Plant-Derived Porous Silicon Embedded in Biocompatible Porous Films

by

Alexa Goehring

Submitted in partial fulfillment of the
requirements of Departmental Honors in
the Department of Chemistry & Biochemistry
Texas Christian University
Fort Worth, Texas

November 30, 2020

A Novel Method for Drug Delivery: Plant-Derived Porous Silicon Embedded in Biocompatible Porous Films

Project Approved:

Supervising Professor: Jeffery L. Coffer, Ph.D.

Department of Chemistry & Biochemistry

Ben Sherman, Ph.D.

Department of Chemistry & Biochemistry

Laura Luque, Ph.D.

Department of Biology

ABSTRACT

Drug delivery is the process by which medications are administered to the body. This is complex due to the difficulty of determining compounds that have the proper biocompatibility and permissibility to our human cells and tissues. Many medications are taken orally; however, there are situations where intravenous injection or subcutaneous delivery is required. Biocompatible porous films are advantageous media for drug delivery as they have low toxicity and high compliance with biological systems. They can also be loaded with drug-containing nanoparticles in an effort to release them into targeted sites. Silicon nanoparticles have unique properties as opposed to bulk silicon; these include biodegradability, larger surface area and biocompatibility. This allows them to be loaded with multiple drugs and alter the release kinetics of each into the biological system.

In this project, porous films were made using two different procedures containing the biocompatible polymer polycaprolactone (PCL were made using two different procedures. The percentage of the polymer in the precursor solution was altered to achieve films with uniform pore size and pore shape. Loading the film with the porous silicon (pSi) allows for two-stage drug delivery and the film was refined by adjusting the percentage of the polymer in the solvent. Physical entrapment and functionalization of the pSi particles were performed to attach them to the depths of the pores to ideally achieve a high percentage pore fill which will maximize drug release. Multiple methods were employed to reduce the aggregations of pSi particles and evaluate the interactions between pSi particles and the porous film. The pSi particles were then loaded with camptothecin (CPT)- a small hydrophobic anticancer drug with fluorescent properties- to detect the drug release kinetics of CPT in pSi particles. This, in addition to evaluating the encapsulation efficiency of CPT, was attempted in an effort to determine the amount of the drug that would be administered via pSi particles in this drug delivery media.

Acknowledgments

This thesis was not possible without the support and aid of many members in the TCU Chemistry Department at TCU.

My utmost gratitude is to Dr. Jeffery Coffer- my supervisor and biggest supporter who has helped me the most throughout the past year and a half in the laboratory. His constant help and words of encouragement have helped me through the many obstacles and have instigated my passion for research. The environment he has created in his research group is very positive and I feel so lucky to have been a part of it.

I would also like to provide my gratitude to Will for taking on the role of my graduate mentor and for always being happy to help me. I am very lucky to have him guide me in the endeavors in this laboratory and for the sacrifice of his time to help me. Nguyen has also helped me whenever I have needed something, and I am grateful for her time and thoughtfulness.

Lastly, I would like to thank my family and friends for being there for me through the ups and downs of my life. To my parents who have supported me emotionally and financially for the past 21 years and have always made sacrifices for my well-being. A huge thank you to my siblings for always pushing me to my best and challenging me constantly. I am very appreciative of everyone who has been there for me and helped me overcome the obstacles I have faced- without them, this would not be possible.

Table of Contents

List of Figures

List of Tables

1 Literature Review

1.1 Introduction

Sixty-six percent (66%) of adults in the United States use prescription drugs[1] and many take more than one medication. Drugs can be administered in multiple ways including orally, parenterally, via inhalation, etc. A majority of drugs are administered orally but one in five people has concerns about swallowing medication and some have dysphagia, the inability to swallow. Biocompatible porous films have been identified as an alternative method for drug delivery that allows the drugs to be administered subcutaneously or buccally[2]. Thin films are advantageous for targeting diseased sites and increase drug efficacy. They are also versatile as there are many different types of thin films and the structure can be altered to increase the loading of the drug, alter the release kinetics of the drug and can decrease the time it takes to experience a given drug's effects. These films are often composed of biocompatible polymers so they can interact with cells, proteins and tissues without eliciting adverse effects.

Porous Silicon (pSi) and silica have low toxicity, and are biocompatible and biodegradable, which allows them to be administered into a biological system without negative side effects[3]. These particles possess a tunable pore size depending on their fabrication route that can influence drug loading and release. The surface chemistry of pSi is largely responsible for the degradation of pSi in biological systems[4]. It allows for various reactions to occur such as oxidation that dictate the disintegration rates. Due to the ability to load drugs into pSi, they can be loaded into biocompatible porous films and ideally administer drugs to patients via a patch.

This thesis focuses on creating porous films from biocompatible polymers utilizing two different methods: (1) Non-Solvent Induced Phase Separation (NIPS); and (2) Thermally Induced Phase Separation (TIPS). Once this process was completed, the pSi particles were embedded into the pores of the films

utilizing different methods. Aggregation of pSi and extent of pore filling were evaluated after they were embedded into the films. The last chapter of the thesis incorporates the loading and release kinetics of Camptothecin (CPT) in pSi. CPT is a model for topoisomerase I inhibitor[5] and its intrinsic fluorescence allows sensitive detection of its release from pSi.

1.2 Porous Silicon

1.2.1 Uses of Porous Silicon

Porous Silicon was discovered in the 1950s and began to be utilized in the semiconductor industry in the 70s[4]. One of the first uses was as a model of the crystalline silicon surface in spectroscopic studies and as a dielectric layer[4]. Silicon has no photoluminescent properties because of its indirect bandgap. Nanostructured pSi has an enlarged band gap thus allowing red orange photoluminescence[6]. This increased its popularity as it had the potential to be incorporated into optoelectronic devices. Practical electroluminescent devices are challenging to produce but progress in luminescent stability may yet improve these applications[7]. Examples of these types of devices are photovoltaic cells, sensors and optical switches.

In addition to visible luminescence properties, other unique features have been discovered as well: large surface area, alterable surface chemistry and biocompatibility[8]. These properties have allowed them to be incorporated in cell membrane-derived vesicles. These vesicles promote the secretion of pro-inflammatory cytokines and the expression of costimulatory signals[9]. These features also led to its usage in drug delivery schemes. PSi has become a good carrier for medicinal drugs due to their controlled drug release to biological systems without eliciting adverse effects[10]. They also can ideally load multiple drugs into a platform that permits patients to take one medication that is loaded with multiple drugs as opposed to many separately.

1.2.2 Porous Silicon Fabrication Methods

There are dozens of fabrication methods for pSi, but the two most commonly used methods are electrochemical etching and chemical etching. In electrochemical etching, pSi is immersed in hydrofluoric acid (HF) to remove surface oxides and impurities. The etching on one side of a silicon wafer uses an apparatus that consists of a copper sheet at the anode with a silicon wafer on top of it and platinum at the cathode[11]. There are other metals besides platinum that can be placed at the cathode. An etching solution consisting of diluted HF and ethanol comes into contact with the top side of the silicon wafer. HF is a common electrolytic solution and ethanol allows for deeper penetration of HF into the hydrophobic silicon surface[12]. A voltage source is used to control current density during the etching process which creates the porous layer in the silicon and the samples are evaluated using imaging by a Scanning Electron Microscope (SEM). **Figure 1** shows a depiction of a simple lateral electrochemical etching setup.

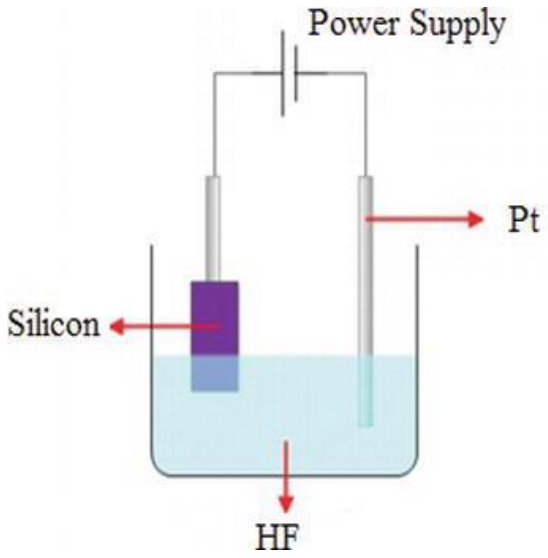

Figure 1. Simple lateral electrochemical etching setup for fabricating pSi[13]

PSi can also be formed via chemical etching which is also referred to as the Metal-Assisted Chemical Etching (MACE) of silicon. The exact mechanism is debatable, but it likely proceeds through electrochemical and mass transport reactions. In this mechanism, the oxidant is reduced on the surface of

the catalytic metal which causes the extraction of electrons leading to holes in the silicon. These holes which are now depleted of electrons can be etched utilizing the electrolytic solution of HF[14].

In this thesis research, anodized pSi was not used, but rather plant-derived porous silicon (pdpSi) which originates from the nodal joints of bamboo plants, a substance known as tabasheer. The purification, advantages and properties of pdpSi will be discussed in the following sections.

1.2.3 Plant-Derived Porous Silicon Fabrication

Porous silicon that is derived from plants acts as an eco-friendly drug delivery matrix and is cheap and efficient to fabricate. The plant that was used for the fabrication of the pSi in this paper was the bamboo plant. Other plants that can be used are sugarcane, grasses and rice[15]. These plants can convert silicon from the soil into nanoporous silica which is an oxide of silicon in the nodal joints of the plant. The anatomy of a typical bamboo plant is shown in **Figure 2**.

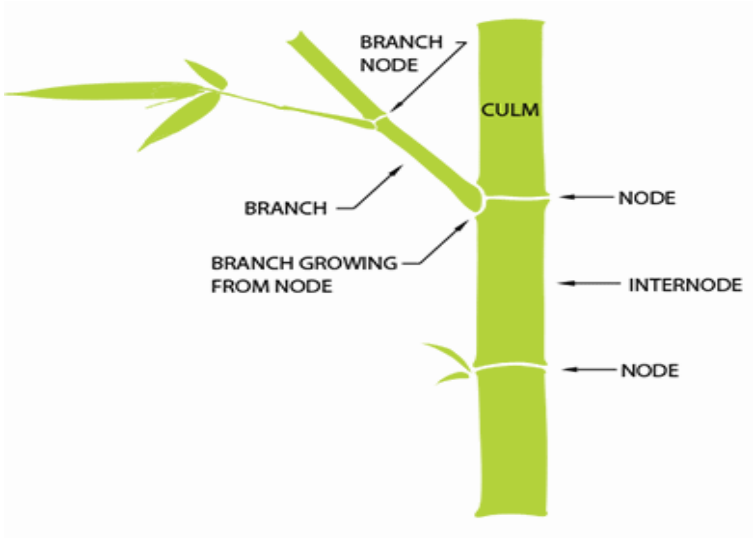

Figure 2. Bamboo Plant Anatomy[16]

Nanoporous silica makes up the majority of tabasheer powder which is a translucent white powder. To extract and purify the nanoporous silica, a five-step process is applied which is visualized in **Figure 4**. The first step includes grinding the tabasheer powder into finer particles, then washing with hydrochloric

acid (HCl) to remove impurities, and collect the product. Calcination is performed to burn off the organics and extract the silica from the tabasheer powder. Magnesiothermic reduction of silica is performed to obtain silicon at $650°C$. Magnesium is oxidized while silica is reduced leading to the products silicon and magnesium oxide shown in **Figure 3**[17].

$$2Mg(g) + SiO_2(s) \rightarrow 2MgO(s) + Si(s)$$

Figure 3. Magnesiothermic Reduction of Silica to form Silicon[17]

An unwanted byproduct is magnesium oxide which deteriorates the purity of the product, so an additional etching step is employed after this using HCl. Washing silicon with HCl to remove the traces of magnesium is the last step of purifying pdpSi and can be confirmed by energy dispersive x-ray (EDX) spectroscopy. This technique is used to identify the elemental composition of materials in the SEM.

Figure 4. Visual representation of pdpSi purification (adopted from Hailey Budensiek)

1.3 Drug Delivery

1.3.1 Methods of Drug Delivery

Drug delivery refers to the process of administering a pharmaceutical compound to achieve a therapeutic event in a living system[18]. The method of drug delivery impacts the amount of time it takes for the drug to be absorbed into the system. The fastest acting methods are injection and inhalation as the drug is either injected into the bloodstream or is inhaled allowing the drug to easily diffuse into the bloodstream and some can be delivered to the brain (if they are able to cross the blood-brain barrier). Methods that take

a lot longer are rectal and transdermal, as they do not have a direct route into the bloodstream. There are limitations to fast-acting methods which often include affordability and concerns with self-administration. Other methods of drug delivery involving the use of nanotechnology in these systems are undergoing investigation. Loading drugs into nanoparticles provide an advantage as they can be transferred into aerosols[18], target specific populations of cells, improve drug efficacy, experience prolonged circulation and improve drug localization[19].

1.3.2 The Benefits of Porous Silicon in Drug Delivery

Leigh Canham demonstrated the biocompatibility of pSi and was the first to promote its usage in vivo[20]. Its first reported use in drug delivery was delivering insulin across the monolayers of Caco-2 cells[21]. The results of that study stated that utilizing the pSi particles had increased the transport of insulin across the monolayers by 25%[21] which led to more studies of utilizing pSi in drug delivery applications. Nanostructure pSi has an advantage over bulk silicon (which is bioinert) because cells adhere to it readily[22]. PSi also has low toxicity and is biodegradable which is an important feature for in vivo usage. The surface chemistry is most important when determining the degradation rate as anodized pSi is covered in reactive hydride species[21].

Multiple ways are still being explored to load and house a drug in pSi. Covalent attachment has been used in biosensor applications but can also be applied to attaching drugs to pSi[10]. Organic drugs that contain a carboxyl species on the end of a terminal alkene may undergo hydrosilylation with Silicon which will result in an Si-C bond[23]. The Si-C bonds in the drug tend to be more stable than Si-O bonds as they are less susceptible to nucleophilic attack.

Other methods to load drugs into pSi are possible via oxidation and even spontaneous methods such as ionic adsorption. When oxidizing silicon into silica, the volume expansion will shrink the pores which can trap any drug particles inside of them shown by (**Figure 5**)[24]**.**

Figure 5. A visual representation of the oxidation of silicon to silica as a method to entrap drug molecules[24]

Simple adsorption is also used to load drugs into pSi particles which can be done by placing the particles into a solution of the drug. Because pSi has a hydrophobic surface, it can absorb small hydrophobic molecules such as CPT, porphyrins, bovine serum albumin (BSA) and more[25]. The plant-derived pSi particles used in these experiments possess an oxide-terminated hydrophilic surface so the hydrophobic fluorescent drug CPT loaded in this manner will not likely generate longer release periods.

1.4 Biocompatible Polymers

1.4.1 Uses of Biocompatible Polymers in Drug Delivery

Biodegradable polymers made from polyesters were first used for biodegradable sutures[26]. Some examples of polyesters that are used as biocompatible polymers are polylactic acid (PLA), polyglycolic acid (PGA) and polycaprolactone (PCL). Since then, they have been incorporated in drug delivery devices as they improve patient compliance and have low toxicity. The degradability of these polymers reduces the need for removal. With large implants, biodegradable polymers can be a problem if toxic byproducts of degradation accumulate; however, many of the ultimate degradation products of biodegradable polymers are ideally carbon dioxide and water[26]. Many polymers are also too stiff and may not be integrated successfully into soft tissue[27]. For this reason, elastic biocompatible polymers became an appealing option. These properties allow them to be incorporated into soft tissues while still having the ability to alter polymer degradation rates. When integrated into drug delivery devices, they can be immersed and degraded safely

in a biological environment without eliciting adverse effects but also can host the drug effectively and control the release of that drug into the surrounding environment. There are multiple ways that biocompatible polymers can be utilized in drug delivery: swelling controlled devices, diffusion-controlled systems, and particulate systems.

Swelling controlled devices (**Figure 6**) are made of cross-linked polymers that have reactive functional groups. These devices are hydrogel based which is a subset of polymers that house large amounts of water (hence the name) and can be cross-linked in the presence of ions. These hydrogels will break when they are swollen which will happen when they are significantly hydrated and release drugs[28].

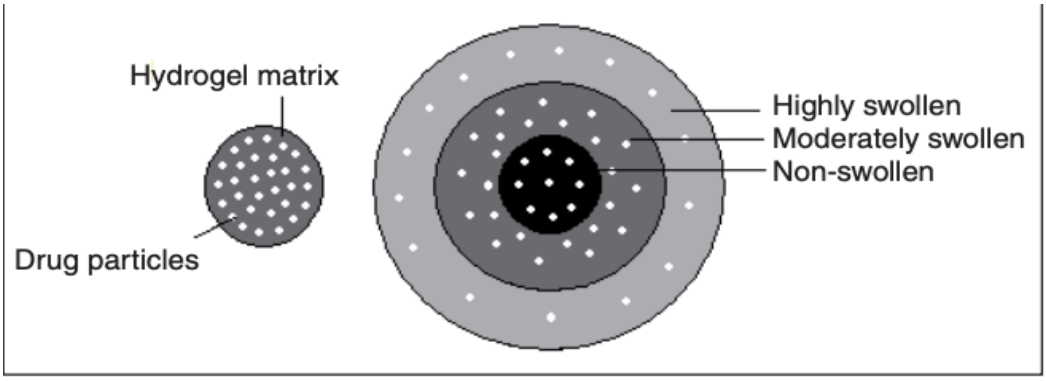

Figure 6. Swellable matrix with drug particles[28]

Diffusion controlled systems deliver drugs via the passive movement of drug particles through the porous membrane into the surrounding environment. The diffusion coefficient is dependent on the polymeric material and whether the membrane is a planar or cylindrical membrane[29]. Each method is versatile and has the potential to be effective to deliver drugs in vivo.

1.5 Methods of Fabricating Porous Films

Non-solvent induced phase separation (NIPS) is a technique that is utilized to make porous films using a polymer and a di-solvent system. A good solvent with higher polymer solubility such as dimethyl sulfoxide (DMSO) is mixed with dichloromethane (DCM) which is a non-solvent with lower polymer

solubility. Upon casting, areas of high polymer concentration form with areas of low/no polymer nearby with only the non-solvent. The polymer crystallizes around the non-solvent leaving porous areas (shown in **Figure 7**). This leads to a film with a diverse, asymmetric pore structure. The asymmetry of the structure does not refer to pores that are asymmetrical when comparing them to each other but refer to the asymmetry of both sides of the films. One side will contain pores while the backside of the film will be flat.

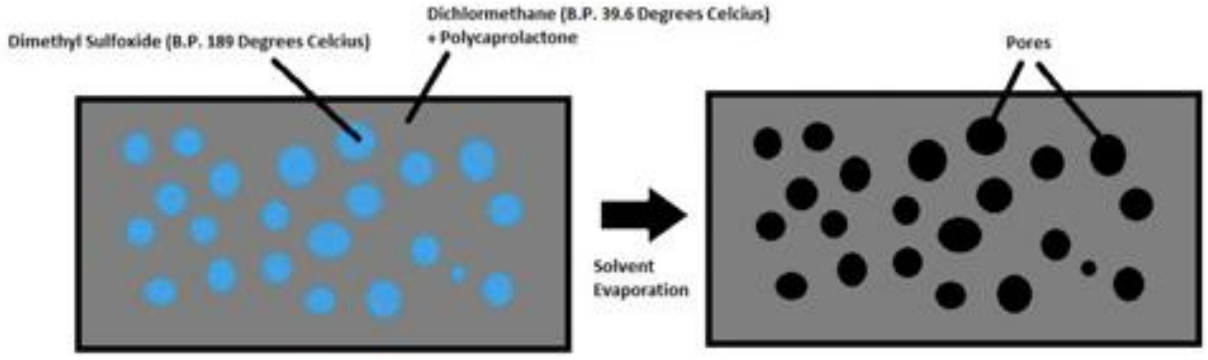

Figure 7. Illustration of the Porous Film that was cast via the NIPS produce

Thermally Induced Phased Separation (TIPS) is another method to form porous films and is advantageous for scaffold preparation as well as interconnected porous structures. The process is done by decreasing the temperature which induces the de-mixing of the homogeneous polymer solution. The homogeneous solution separates into polymer-rich and polymer-less phases creating pores.

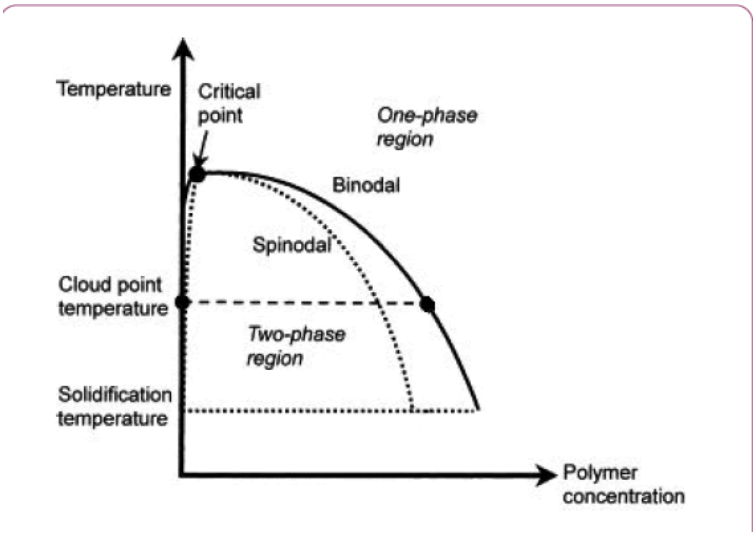

Figure 8. Visual Depiction of TIPS Film Formation[30]

Figure 8 is a visual representation of the process; the region between the binodal and spinodal curves is where the growth occurs, thereby, creating large pores. The region below the spinodal line occurs faster and represents the separation mechanism which creates smaller interconnected pores.

Since temperature is responsible for the formation of the pores, only one solvent is needed, which was DMSO. The glass plate is placed over dry ice and the solution of PCL and DMSO is poured onto the plate and spread with a razor blade. To adjust the pore size, temperature and time can be changed. As temperature and time both increase, the Feret's diameter of the pores, which is the longest distance between the edges of the pores, also increases (**Figure 9**).

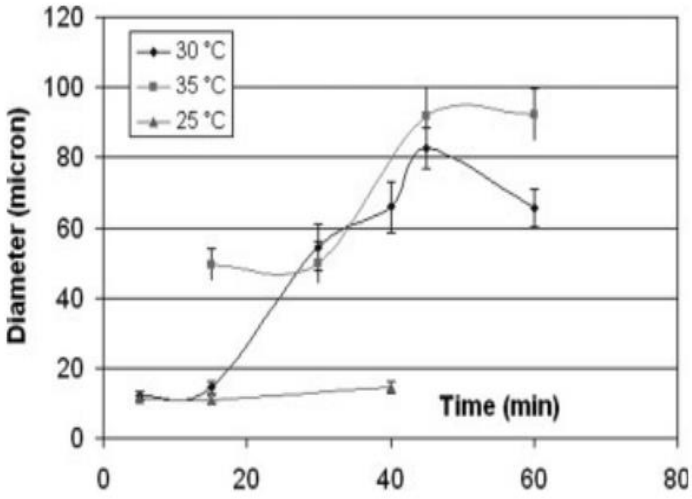

Figure 9. The Effect of Time and Temperature on TIPS Films[30]

2 Creating Polymer Porous Films Integrated with Porous Silicon for Drug Delivery

2.1 Introduction

Porous polymer films can be constructed using various methods such as Non-Solvent Induced Phase Separation (NIPS) and Thermally Induced Phase Separation (TIPS) discussed in the previous chapter. In this chapter, both of these methods have been evaluated to determine which one results in films that have relatively more uniform pores that are size-tunable. Being able to adjust the pore size is important when deciding what particle size of porous Si (pSi) will be loaded inside the pores of the polymer. The percentage of polycaprolactone (PCL) in the di-solvent system of DCM to DMSO, along with the ratio of these two solvents were adjusted to achieve this goal. PCL is a hydrophobic polyester that is biodegradable, biocompatible, inexpensive and approved for tissue engineering by the FDA[31]. The films were evaluated by utilizing Scanning Electron Microscope (SEM) imaging to visualize the structure of the pores and evaluate the Feret's diameter of each pore and associated, standard deviation.

Once the best ratio of PCL to DCM/DMSO was determined, I experimented with entrapping plant-derived porous silicon into the depths of the pores. The first method I tried was physically entrapping the porous silicon in the films. Two methods could achieve this: (1) adding the porous Silicon to the PCL dissolve in DCM/DMSO before casting the film. Another method was suspending the pSi in distilled water, then spreading the mixture onto the already casted film. Due to the results of the physical entrapment, I attempted to covalently bind the plant-derived porous Si (pdpSi) to the bottom of the pores. This procedure utilized the functionalization of these particles with (3-Aminopropyl)triethoxysilane (APTES) (evaluated by Zeta Potential measurements) then followed by exposure to glutaraldehyde (GTA). These particles were mixed with phosphate-buffered saline (PBS) then spread on the films and left to dry overnight before evaluating the deposition of the pSi. To decrease the aggregation of pSi on the surface of the films and increase the deposition in the pores, four methods were employed. The first one was utilizing horn sonication

to ideally evenly distribute the particles in phosphate-buffered saline (PBS). Another was lightly going over the surface of the film in the presence of the pSi particles with a razor blade to reduce aggregation. Spraying the film with nitrogen gas to remove the porous silicon from the film was the third method that was attempted. Finally, the last method was dipping the film in water with the pSi embedded in the pores in water. The percentage of pores filled and ultimately retained by each method was evaluated using SEM imaging.

2.2 Experimental

Instrumentation

- Scanning Electron Microscope (SEM)- JEOL Model: 7100F
- Zeta Potential- Brookhaven Instruments EN 60825-1:2001
- Fluorescent Spectrophotometer- Agilent Model: Cary 60
- Horn Sonicator- Branson Sonifier Model: 450

Procedures

NIPS was used to make porous films utilizing the biocompatible polymer PCL and the two solvents DMSO and DCM. The solutions consisting of PCL and 10 milliliters of the combined solvents were spread on a glass plate that was ~7x8 inches and spread with a razor blade, then left to dry. This procedure was used in combination with mixtures that ranged from 20 to 35% weight by weight PCL in 8:2 and 9:1 ratios of DCM to DMSO. These films which were ~3x6 inches resulted in pores that ranged from 2 to 12 microns in diameter. SEM imaging allowed visualization of the films to evaluate the uniformity of the pores and crystallization around the non-solvent.

After it was decided that the three films made with the NIPS technique yielded the best results, placing the pdpSi into the depths of the pores was then attempted. The first method was physically entrapping the pSi in the polymer which was done by adding the pSi into the mixture of PCL, DCM and DMSO before the film was cast then was spread on the film. To increase the deposition of pSi within the

pores, another technique employed casting the films, then mixing the pSi with distilled water and spreading them on the film.

Covalent attachment of pSi particles to the films is ideally a more stable method than physical entrapment. To do this, the pSi first underwent APTES functionalization by being incubated in a 5% solution of APTES in toluene for 2 hours, then was rinsed with toluene and water/ethanol (1:1) before centrifuging the sample to remove the supernatant and left in a vacuum to dry. This reaction involves modification of the ethoxy groups on APTES into hydroxyl groups then undergoes a hydrolytic condensation with silanol groups of pSi[32] (**Figure 10, A**). Fluorescein isothiocyanate (FITC) conjugation with APTES functionalized pSi was performed (**Figure 10, B**) to provide a fluorescent probe of evidence of functionalization.

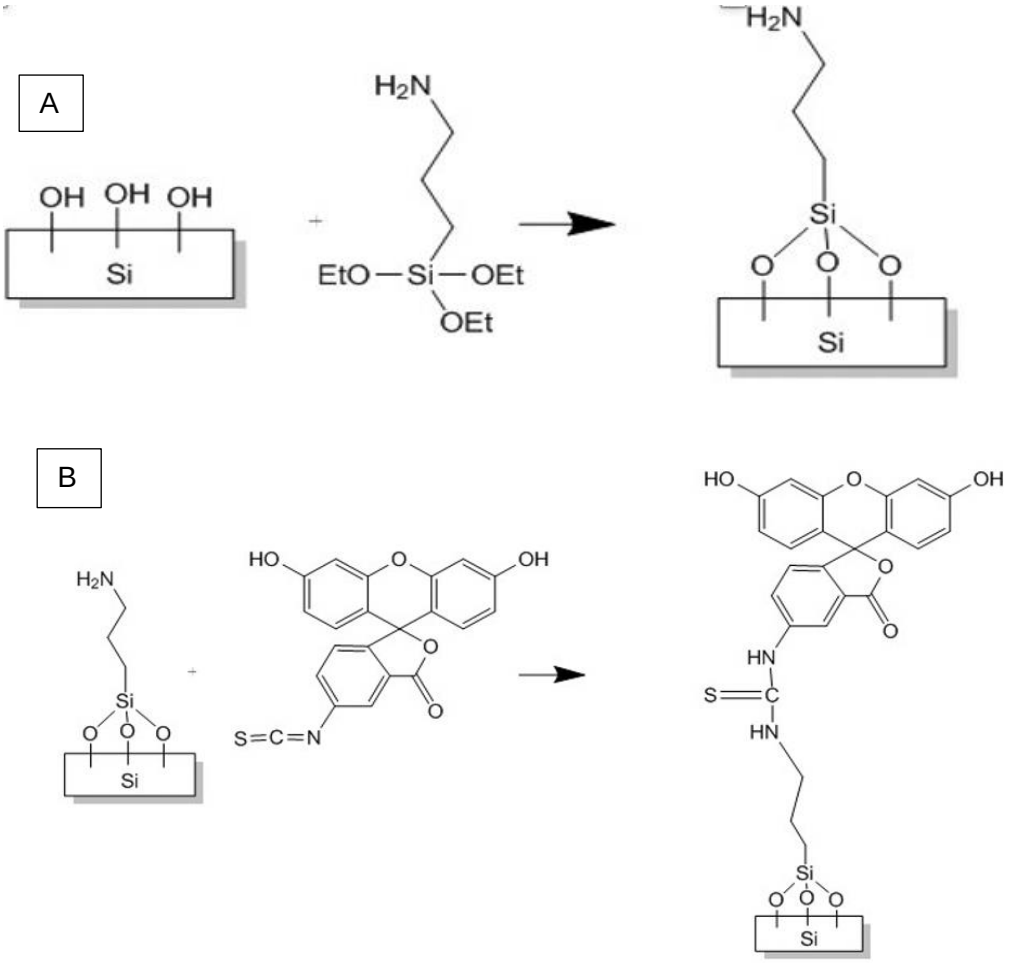

Figure 10. The reaction between silicon and APTES (A: top, B: bottom)

Another test of functionalization is the zeta potential measurements. Zeta potential measures the surface charge of particles by tracking the rate at which charged particles move in response to an electric field[33]. Particles of a positive charge move to a negative electrode and vice versa. The rate of the movement is proportional to the zeta potential of the material being measured (surface charge). The absolute magnitude of the charge is less important than the sign, as the surface charge of the particles should be positive after functionalization due to the amine group; a low standard deviation as a low standard deviation provides confidence in the zeta potential value.

Table I. The results of the zeta potential value of the APTES Functionalized pSi particle

Run	**Mobility**	**Zeta Potential (mV)**	**Rel. Residual**
1	1.10	14.07	0.0254
2	0.97	12.42	0.0161
3	0.95	12.19	0.0111
4	1.19	15.21	0.0177
5	1.20	15.32	0.0233
6	1.14	14.65	0.0238
7	1.19	15.20	0.0124
8	1.20	15.38	0.0216
9	1.10	14.08	0.0190
10	1.05	13.38	0.0227
Mean	1.11	14.19	0.0193
Std. Error	0.03	0.38	0.0015
Combined	1.11	14.19	0.0077

After APTES functionalization of the particles, glutaraldehyde (GTA) functionalization was performed (**Figure 11**). The pSi particles were inserted in 2.5% glutaraldehyde in PBS and rinsed with PBS before centrifuging the sample and removing the supernatant then dried in a vacuum overnight.

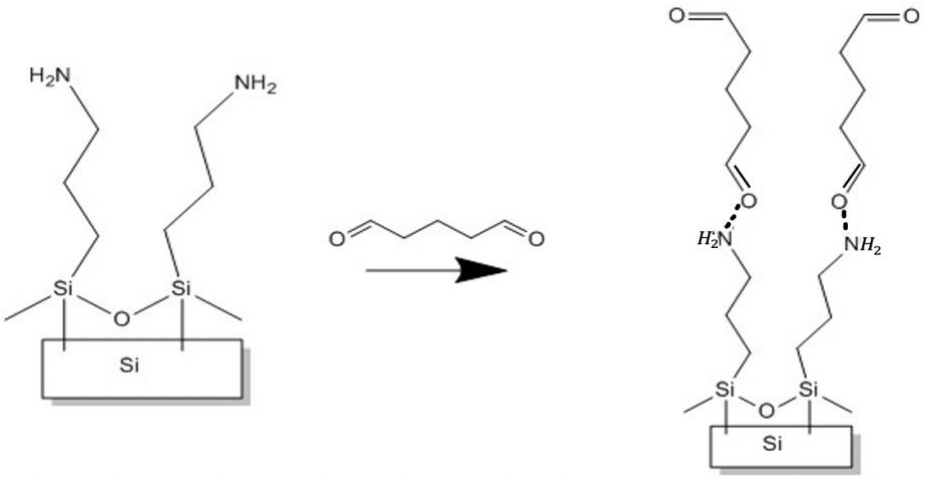

Figure 11. Reaction scheme of GTA functionalization of APTES functionalized pSi particles

Water was also utilized in the place of PBS as a control to evaluate the role of salts in PBS. Once this was done, these particles were mixed with water in a 1:2 ratio and spread on films.

Suspending the pSi on the surface of the films led to films with aggregated pSi particles on the surface and not at the bottom of the pores. To reduce the aggregates and increase deposition, four methods were employed. The first was utilizing the horn sonicator to more uniformly disperse the pSi in the water using ultrasonic radiation which operates at 20kHz. The duty cycle was 4 or 5 which altered the length of each pulse.

The next technique was gently physically scraping the film with a razor blade after the functionalized pSi particles were already added to the film, which led to disruptions in the pore morphology. Spraying the film with the pSi particles already on it with nitrogen gas was another method used to try to reduce the loose number of pSi particles on the surface. This method will also determine if the pSi particles have a strong interaction with the film or if they all are removed upon spraying nitrogen

gas onto the film. The last method that was used was dipping the dry films that already contained functionalized pSi particles in water. Before dipping, aggregated pSi were present on the surface. To make sure particles were composed of Si, Energy dispersive x-ray analysis (EDX), which can identify (in the SEM) the elemental composition of a film (**Figure 12**) was performed.

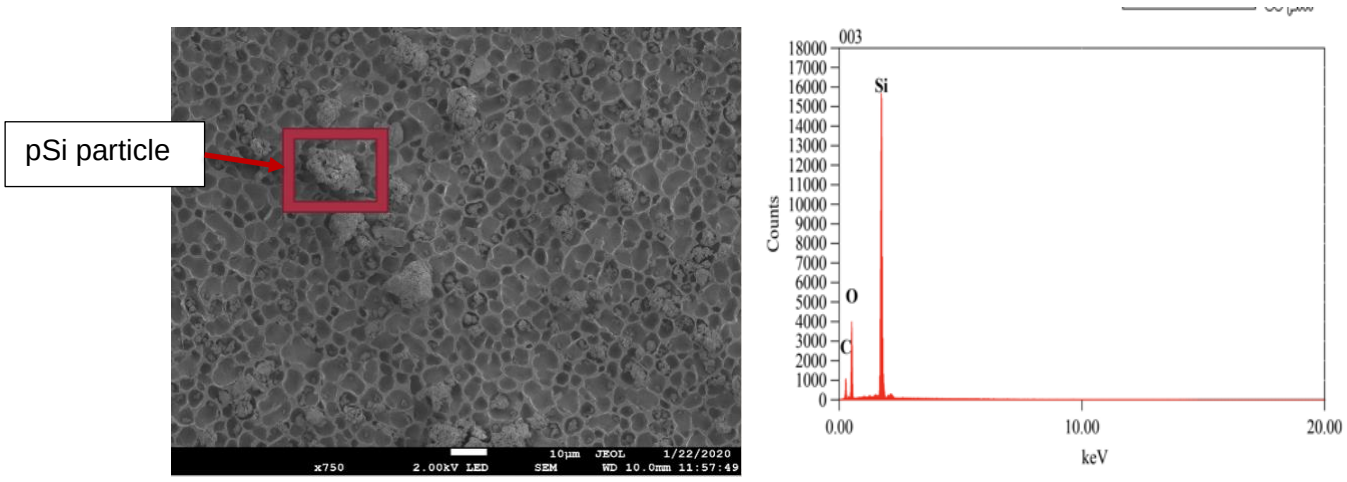

Figure 12. Chemical composition of the particle on the porous film in the image (A) utilizing the EDX (B)

Table II. The mass percent of Silicon of the particle on the film in Figure 12

Element	Mass Percent
C	27.36
O	36.37
Si	36.27

Each of these deposition techniques was evaluated to determine the best one to reduce aggregation, maintain morphology, and increase pore deposition.

2.3 Results and Discussion

Different percentages of PCL in 9:1 and 8:2 ratios of DCM to DMSO were used to make films. In films that were cast from the precursor solution contain a higher percentage of the polymer resulted in pores that were merged represented in **Figure 13**. This means that many of the pores are not distinct from one another creating giant pores instead of many smaller ones.

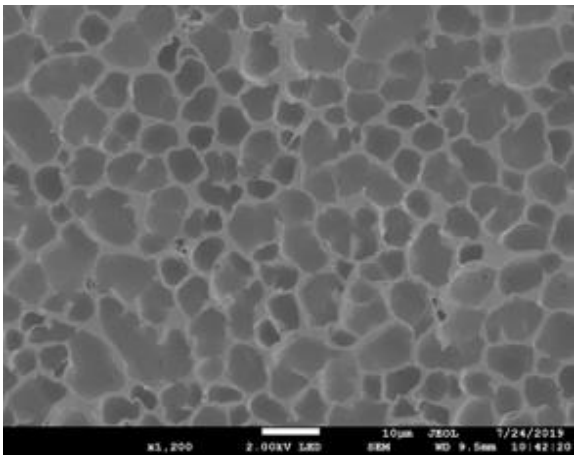

Figure 13. SEM image of a porous film derived from controlled evaporation of a 35% w/w PCL in a 9:1 DCM to DMSO mixture

After attempting to create multiple films, I found that there were three ratios of biocompatible polymer to the solvent that led to distinct, uniform, and relatively symmetrical pores. These three films were 25% w/w PCL in 9:1 DCM to DMSO, 30% w/w PCL in 9:1 DCM to DMSO and 25% w/w PCL in 8:2 DCM to DMSO. These were chosen because of the low and consistent standard deviations and the uniform pore structures of the films. In the SEM images of the films, the bar at the bottom of the image represents the scale bar and is used to measure the Feret's diameter of the pores.

Table III. Influence of PCL Concentration in 9:1 DCM to DMSO on Pore Size

Weight Percentage of PCL in DCM to DMSO	**Average Pore Size (microns)**	**Standard Deviation (microns)**
25 (film 1)	9.69	3.51

25 (film 2)	11.76	3.70
30	5.62	1.40

Table IV. Influence of PCL Concentration in 8:2 DCM to DMSO on Pore Size

Weight Percentage of PCL in DCM to DMSO	**Average Pore Size (microns)**	**Standard Deviation (microns)**
25 (film 1)	4.08	2.64
25 (film 2)	2.49	1.02
34.66	7.91	4.17

While the films made of 25% w/w PCL in 9:1 DCM to DMSO (**Figure 14**) had a higher standard deviation than the others, the pores were of similar shapes and led to distinct pores as opposed to merged ones.

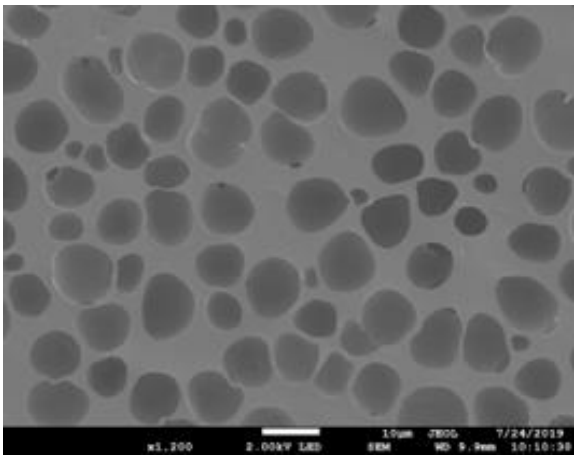

Figure 14. SEM image of a porous film derived from controlled evaporation of a 25% w/w PCL in a 9:1 DCM to DMSO mixture.

The film made with 25% w/w PCL in 8:2 DCM to DMSO (**Figure 15**) had a lower standard deviation overall in regard to pore size consisting of many smaller pores that were less than a micron size in between the larger ones typically 2 to 3 microns in size.

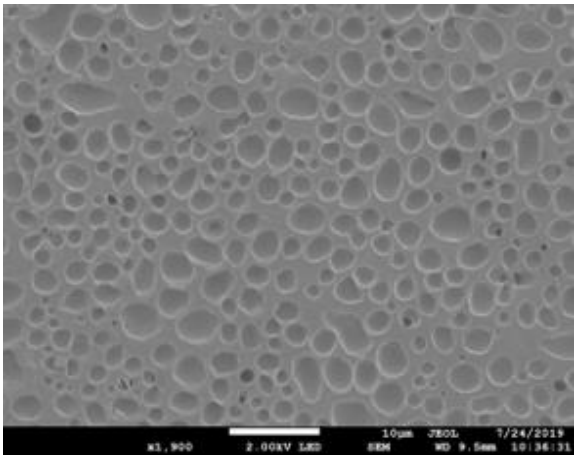

Figure 15. SEM image of a porous film derived from controlled evaporation of a 25% w/w PCL in a 8:2 DCM to DMSO mixture.

The last combination was 30% w/w PCL in 9:1 DCM to DMSO which resulted in a low standard deviation of pore size and distinct pores (**Figure 16**). While these films did not have merged pores, they aggregated near each other leaving large non-porous areas.

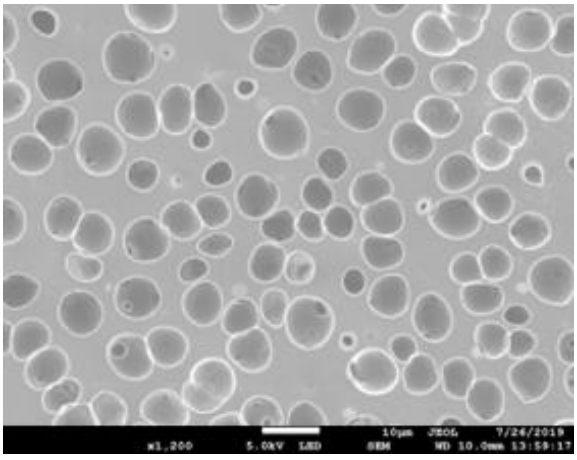

Figure 16. SEM image of a porous film derived from controlled evaporation of a 30% w/w PCL in a 9:1 DCM to DMSO mixture.

When using the TIPS method to make films, I found that films cast at 21°C led to pore sizes that resulted in less than a micron and films that cracked easily when drying (**Figure 17**).

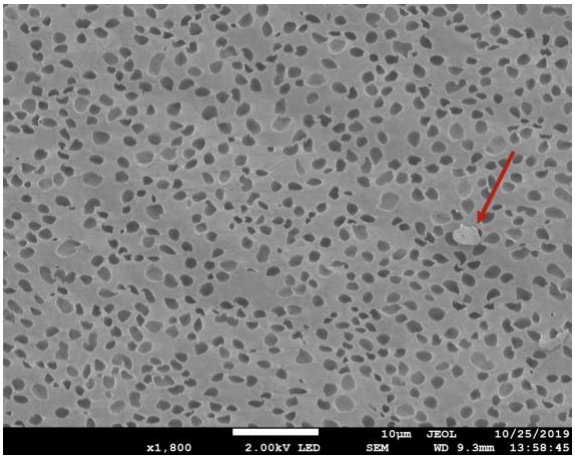

Figure 17. SEM image of a porous film casted via the TIPS procedure with pSi on the surface (red arrow).

The films that were made at 7°C led to the formation of spherulites (**Figure 18**). Spherulites are semi-crystalline spherical structures inside linear polymers. Spherulites form from polymeric materials during periods of large undercooling which is shown in **Figure 19**.

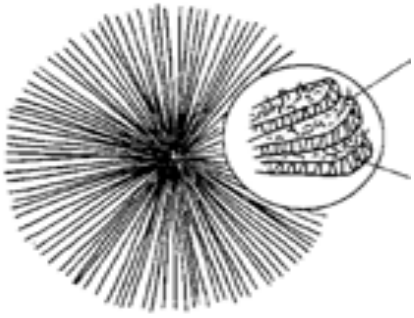

Figure 18. Spherulites[34]

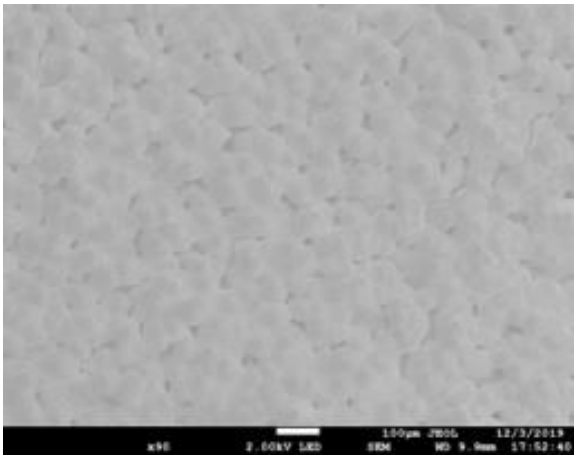

Figure 19. SEM image of a TIPS film prepared at 7°C resulting in the formation of spherulites

Because of these results, NIPS was determined to be the best method for film casting. The next phase when incorporating the pSi into the pores which were done by covalent attachment and physical entrapment. When attempting to physically entrap the pSi by adding them to the solution before casting the film, the pSi was widely dispersed on the films and not deposited deep into the pores. Many of the films had areas with no pSi particles (**Figure 20**) or a very minimal amount. These results suggested that physically entrapping the pSi was not an effective method for pSi particle deposition in the pores of a given film.

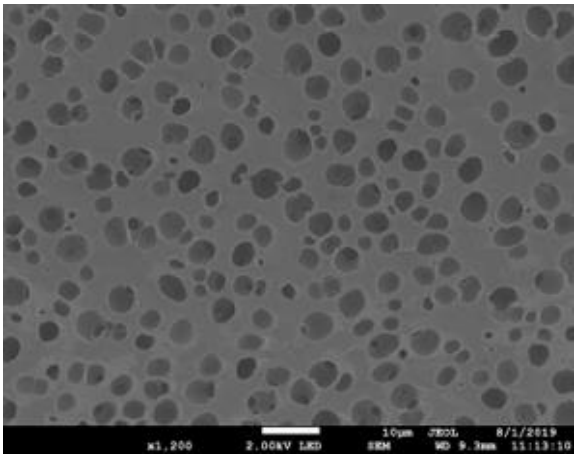

Figure 20. SEM image of a porous film with physically entrapped pSi that resulted in large areas with no pSi particles present.

However, covalently binding these particles to the films was a possible solution to this. APTES functionalization was performed and upon analysis of zeta potential, it was a success as the particles were positively charged due to the addition of the amine group. The additional treatment of glutaraldehyde led to interactions between the amine group and the aldehyde but it likely did not lead to a covalent linkage. Coupling agents such as dicyclohexylcarbodiimide (DCC) would need to be added to form a covalent linkage between the polymer and the amine group. The carboxylic acid group of PCL will form a carboxylate ion and it will be coupled with the primary amine to form an amide in the presence of a coupling agent as carboxylates are very unreactive. The interactions in this project are likely electrostatic which would easily be disrupted in the body by salt. Ideally, coupling agents would be added to this step of the procedure to promote a covalent linkage.

The films treated by this APTES/GTA route were analyzed via SEM, the pSi particles were very aggregated on all of the films (**Figures 21 and 22**).

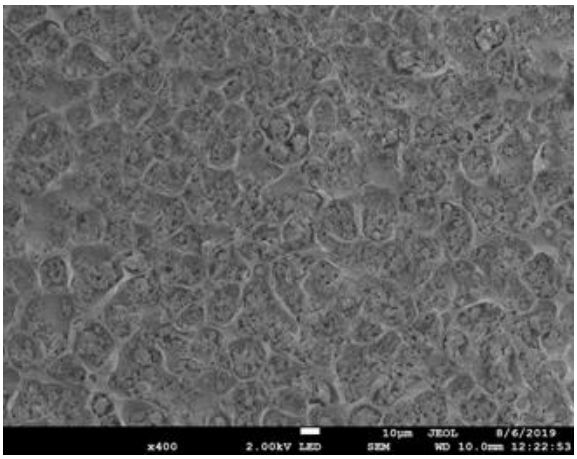

Figure 21. SEM image of a porous film derived from controlled evaporation of a 25% w/w PCL in a 8:2 DCM to DMSO mixture with APTES/GTA functionalized pSi.

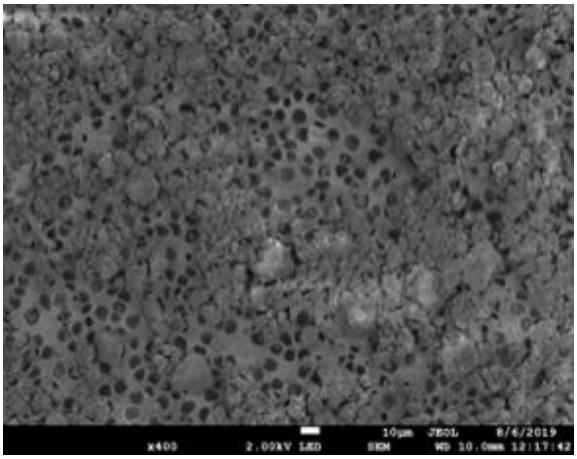

Figure 22. SEM image of a porous film derived from controlled evaporation of a 30% w/w PCL in a 9:1 DCM to DMSO mixture with APTES/GTA functionalized pSi.

To reduce this, a horn sonicator was used to disperse the pSi in water and then spread across the porous polymer. This resulted in particles that were less aggregated but there was a decrease in pore deposition, about 5.6% pore fill which is shown in **Figure 23**. Pore fill is calculated as the number of pores in a given film that contain pSi particles in them. The number of pores with pSi is divided by the total number of pores imaged and multiplied by 100 to calculate the percentage.

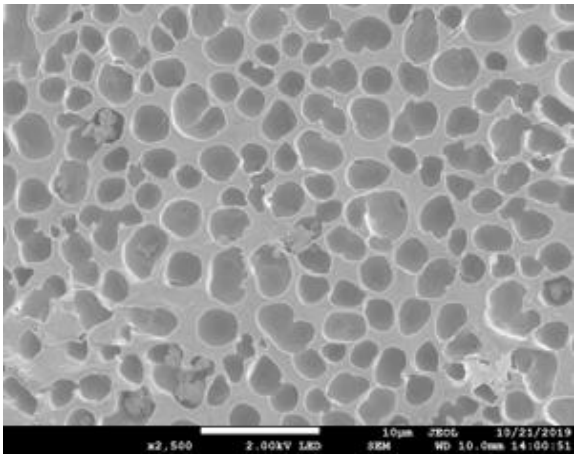

Figure 23. SEM image of a porous film with physically entrapped pSi.

When utilizing a razor blade to prevent the aggregates, it led to the razor blade cutting the film and ripping it as well as pores that were not distinct and now flat (**Figure 24**).

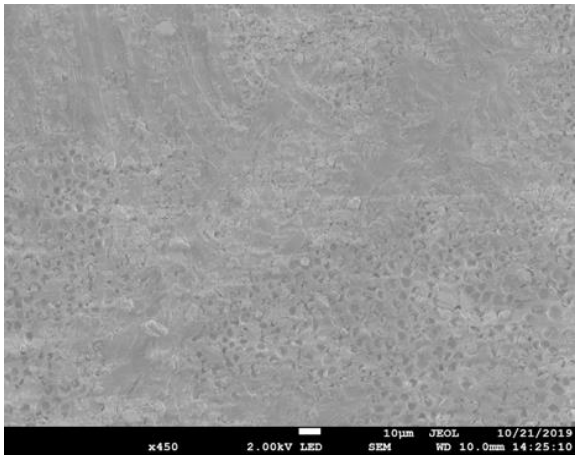

Figure 24. SEM image of a porous film that was gently scraped with a razor blade to remove aggregates of pSi.

When the film was sprayed with nitrogen gas to remove loosely bound pSi aggregates from the polymer surface, the majority of the pSi particles were removed and minimal amounts were deposited into the pores. This can be seen below in **Figure 25** which depicts gray and white pores due to the charge on the surface picked up by the SEM.

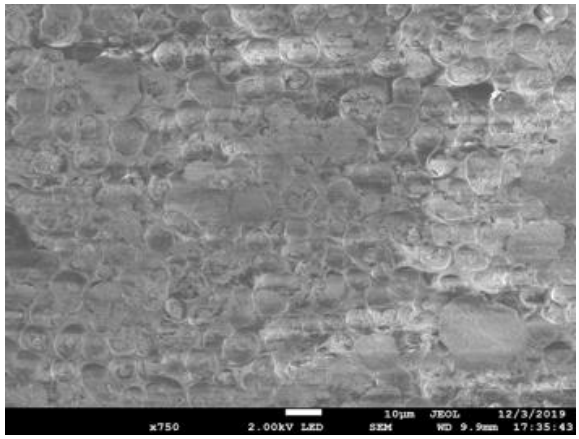

Figure 25. SEM image of a porous film derived from controlled evaporation of a 30% w/w PCL in a 9:1 DCM to DMSO mixture with nitrogen gas sprayed on the polymer surface to reduce pSi particle aggregates.

The last method that was tested involved dipping the porous films in water then analyzing the pSi particle aggregates on the surface. Before this was done, SEM images were taken of the film to determine the effectiveness of this technique. The film before and after it is dipped in water is depicted in **Figure 26**.

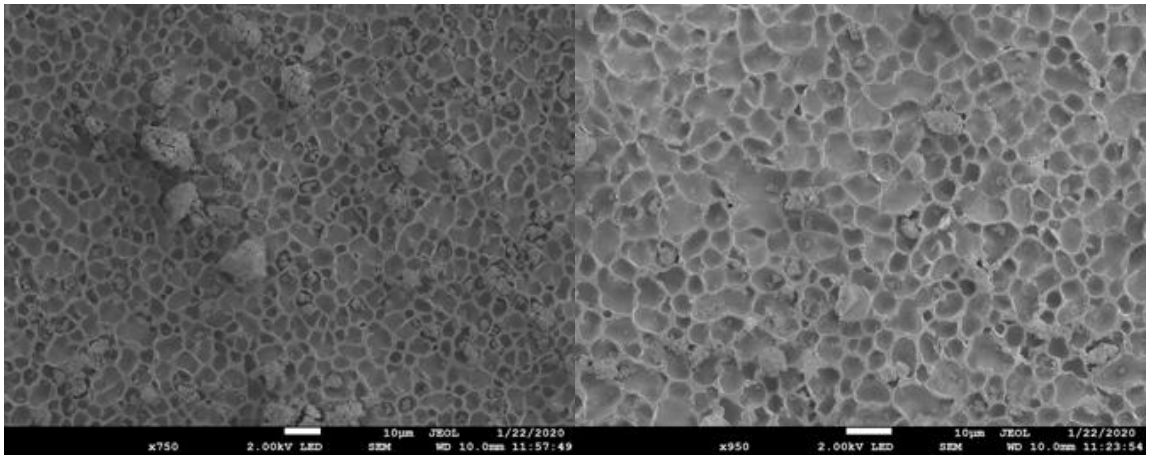

Figure 26. SEM images of porous films with functionalized pSi before (left image) and after (right image) dipping in water.

2.4 Summary

In this chapter, NIPS and TIPS porous film fabrication methods were both utilized to determine the films with consistency in morphology, have a low standard deviation in the ferret's diameter of the pores and symmetrical pore shape. TIPS films led to films that easily cracked and the formation of spherulites as opposed to the NIPS films. When experimenting with the percentages of PCL in two different ratios of DCM to DMSO, 30% w/w PCL in 9:1 DCM to DMSO, 25% w/w PCL in 9:1 DCM to DMSO and 30% w/w PCL in 8:2 DCM to DMSO led to the generation of the pores that fit the desired parameters.

When adding the pSi into the films, physical entrapment led to the sporadic deposition of the pSi so covalently bonding them to the films utilizing APTES and GTA functionalization had more potential. This led to increased deposition of pSi into the pores and on the film. There were many aggregates so four methods were used to reduce the number. Horn sonication was used to mix the particles before distributing them on the film and was not as effective in depositing pSi into the pores. Another method that was not effective was lightly scraping the surface of the film with a razor blade to remove aggregates which resulted in disrupter pore morphology. The two effective methods were spraying the films with nitrogen gas and dipping the films in water. This removed many of the aggregates and particles that were not covalently

attached but left 10-20% pore fill as opposed to the initial 50% pore fill. Composition of most of the imaged particles was confirmed utilizing EDX.

3 Release Profile of Camptothecin from Functionalized Plant-Derived Porous Silicon

3.1 Introduction

The next phase of the project was detecting drug release via the porous film. Camptothecin (CPT) was selected as it is a good model drug for hydrophobic drugs which are more difficult to deliver. This compound (**Figure 27**) also has fluorescent properties that allow it to be detected utilizing fluorescence spectrophotometry. CPT is utilized as a chemotherapeutic as it inhibits topoisomerase I which allows DNA replication to be inhibited[35].

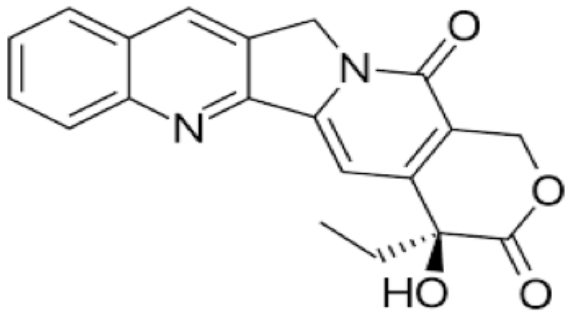

Figure 27. Structure of CPT

CPT was loaded into the pSi particles and the encapsulation efficiency of CPT was calculated as well as the drug release kinetics. The encapsulation efficiency represents the percentage of CPT entrapped in the plant-derived porous Silicon (Equation 1).

(the measured amount of CPT loaded into pSi÷theoretical amount of CPT loaded into pSi)×100 (1)

Before advancing to embedding the functionalized pdpSi into the porous films and detecting the release of CPT, CPT release from the pSi particles needed to be evaluated first. Two different percentages of CPT loading in these particles were evaluated for encapsulation efficiency and the drug release of CPT over time.

3.2 Experimental

The first step was preparing the 0.1mg/mL CPT in DMSO stock solution. This stock solution was used to load the CPT into the pSi particles which was done by incubating the particles in the stock solution and placing them on a Vibrax shaker overnight. The particles were centrifuged and the supernatant was removed before placing the pdpSi into a vacuum to dry overnight to ensure DMSO removal. The volume of the stock solution added was dependent on the desired percentage of CPT loading in the pdpSi particles. 1% w/w CPT in pSi were evaluated first and 2% w/w CPT in pSi were evaluated thereafter.

The drug release kinetics of the first particles were evaluated by placing the loaded particles into the water and the supernatant was evaluated at different time intervals of 1 through 4 or 5 minutes. The supernatants were each added to the well plate and the intensities were evaluated using the fluorescent spectrophotometer which was set to an excitation wavelength of 370nm and an emission wavelength of 430nm associated with CPT. The PMT voltage was decreased if the intensity is greater than 1000 counts as the results are less reliable. Once the intensities of each of the supernatants were evaluated, the calibration curve of CPT in water was utilized to generate a linear equation that was used to calculate the amount of CPT released from the particles.

To determine the encapsulation efficiency in water, the CPT loaded particles were placed in water and centrifuged overnight to ensure full release. The supernatant was collected and the intensity of the supernatant, as well as the calibration curve of CPT in water, was used to determine the amount of CPT released from the particles. The same was done in DMSO as CPT is completely soluble in DMSO so all of the pSi should be released in the media.

The same was done with 2% w/w CPT loaded pSi and the release kinetics were evaluated.

3.3 Results and Discussion

The release of 1% w/w CPT in pSi in water was evaluated first at time intervals of 1-4 minutes. The supernatant of the sample at each time point was collected and the intensity of each was evaluated using the fluorescence spectrophotometer (**Figure 28**).

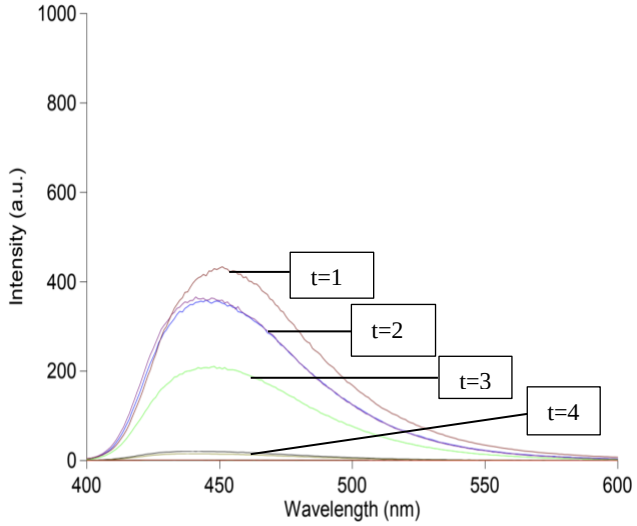

Figure 28. The intensity of 1% w/w CPT in pSi in water at time intervals 1-4

The intensity of CPT fluorescence at each time interval was plotted against time and the R^2 was evaluated which measures the linearity of the fit. In **Figure 29**, the amount of CPT released from the pSi is highest at the beginning of incubation in water which provides insight into in vivo release.

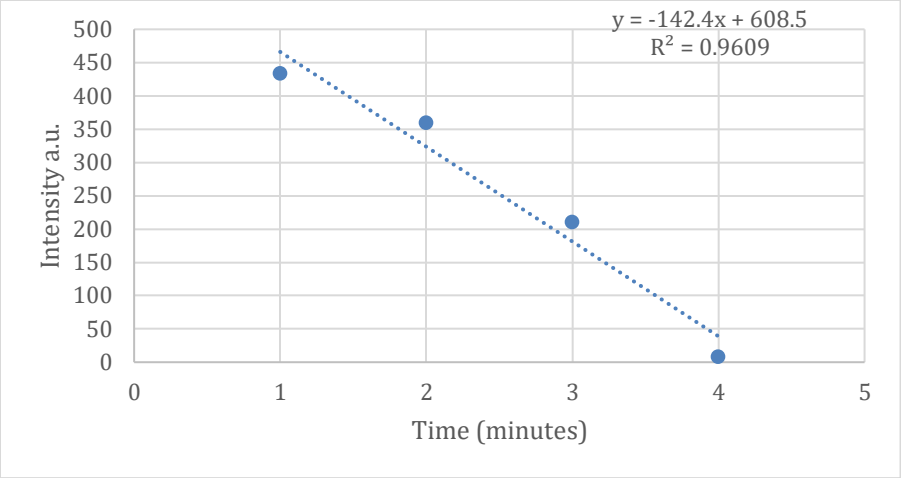

Figure 29. Release of 1% w/w CPT in pSi in the water at time intervals 1-4.

The next step was to calculate the encapsulation efficiency of CPT in water and DMSO which is done using the calibration curve of CPT to water or DMSO to find the amount of CPT released. This value is divided by the total amount of CPT that was loaded and multiplied by 100 to calculate the percentage. When determining the intensity of the pSi particles loaded with 1% w/w CPT, the fluorescence of CPT was below the detection limit of the fluorescent spectrophotometer. This is likely because the loading percentage was so low that the amount of pSi would have needed to be very large to release enough CPT to be detected. To combat this, a larger amount of pSi particles was used as well as the loading percentage was increased to 2% w/w CPT in pSi for the next trial.

The pSi particles were loaded with CPT to achieve 2% w/w CPT in pSi then evaluated from the same time intervals as before (1 to 4 minutes). I increased the amount of pSi used to load more CPT in the particles to achieve a release that ideally would be detectable. However, this did not seem to work as the intensities were lower in this experiment than when utilizing 1% w/w CPT loaded pSi particles. It is possible that the pSi particles needed to be submerged in the CPT solution for a longer amount of time while being continually mixed due to the large number of pSi particles which also tend to aggregate together. Upon evaluating the triplicates of the supernatants from each time increment, I was able to average the intensities

and construct the graph in **Figure 30**. The adjustment that should be made is that the supernatants should be evaluated at longer time intervals. In terms of possible future experiments, I would recommend measuring release until 8 minutes or the time interval in which the intensity of the supernatant is below the threshold as that would conclude that the amount of CPT released is very minimal.

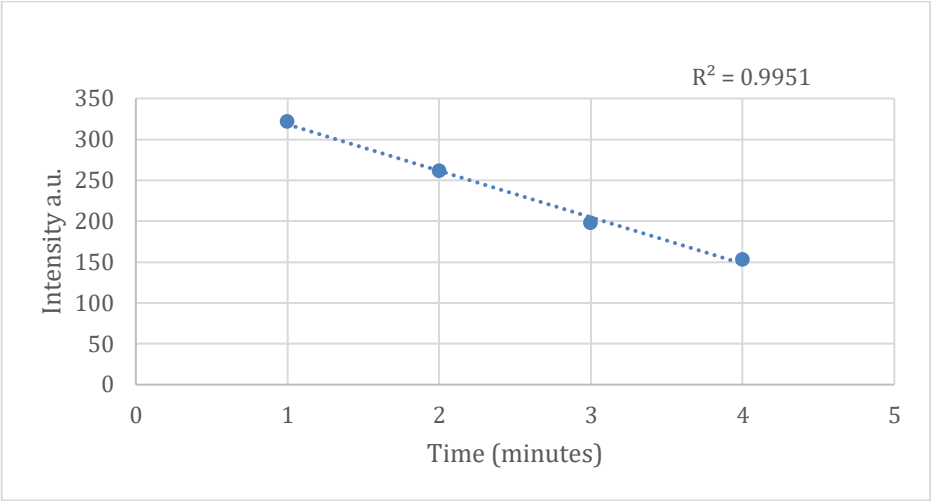

Figure 30. Releasing CPT from 2% w/w CPT loaded pSi particles in water and the corresponding linear regression on the right.

A calibration curve of CPT in water was also constructed using the fluorescent spectrophotometer with the PMT voltage set at 600mV but there were small differences in the intensities of different concentrations (**Figure 31**). The R^2 value was also lower than that of DMSO which is likely because CPT is only partially soluble in water which can lead to insufficient mixing. While I did mix the solution using a micropipette, CPT particles were still visible and could certainly affect the results of the calibration curve.

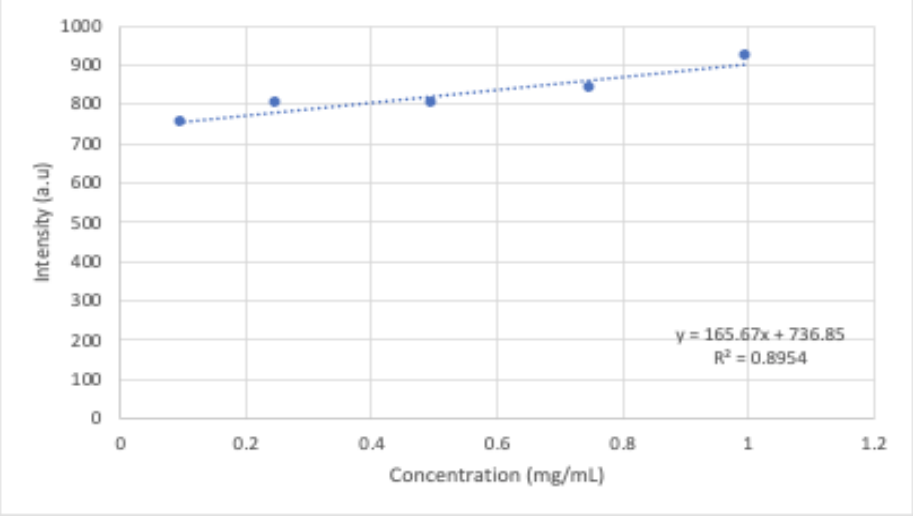

Figure 31. Calibration Curve of CPT in Water at 600 mV.

Figure 32 represents the calibration curve of CPT in DMSO and has a higher confidence value for the linear fit. The point at (0,0) was not necessarily 0 but since it represented DMSO without CPT, the intensity was below the threshold which was set at 25 counts. This is applied to determine the encapsulation efficiency of CPT; however, this has not been done yet and should be evaluated in future work.

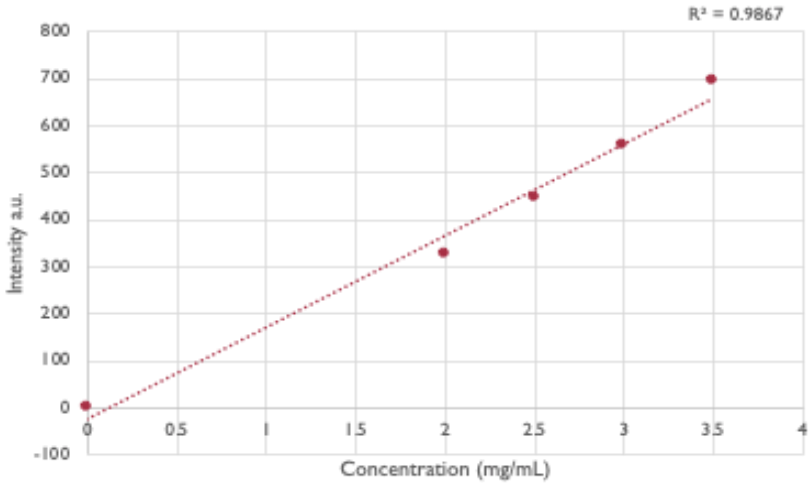

Figure 32. Calibration Curve of CPT in DMSO.

3.4 Summary

When evaluating the results of 1% w/w CPT loaded in pSi particles, it was determined that the quantity of the pSi particles needed to be high to ensure a detectable amount of CPT. **Figure 30** presents the fluorescence intensities of CPT in water and DMSO to determine the encapsulation efficiency but led to intensities under the threshold- 25 counts; A very small amount of pSi particles were used- around 1mg- so the CPT loaded in them was around or less than 0.01mg. A larger amount of pSi particles was used to evaluate the release kinetics in water as an effort to replicate a biological environment and it was concluded that the majority of the pSi was released at time interval 1 and the amount decreased as time went on.

The results of the 2% w/w CPT loaded pSi particles were consistent with that of 1% as the majority of CPT was released at time interval 1 and subsequently decreased. However, the intensity of the supernatants at these intervals was not as high as those that were collected from the experiments with 1% w/w CPT loaded in pSi. This was misleading as the amount of pSi was increased to 18 mg from ~10 mg, however, these particles needed a longer time to soak in the CPT solution and needed to be continually mixed. This should be redone in future experiments. Encapsulation efficiency should also be done to evaluate the percentage of CPT that is released in its environment but should be altered by increasing the number of pSi particles as an effort to achieve a detectable release of CPT. The calibration curves of CPT in DMSO and water assist in determining the concentration of CPT released; however, the calibration curve of CPT in water will also need to be redone. To achieve more accurate dilutions, the dilutions should be put in the horn sonicator before they are transferred to the wells to mix the CPT more uniformly in the water.

4 Conclusion

In this thesis, biocompatible porous films loaded with pdpSi were created as a potential novel method for multi-stage drug delivery. The biodegradability, biocompatibility, surface area and efficiency of this platform increases the appeal to explore this method for administering medications. PdpSi is eco-friendly, cost-effective and abundant in nature while also maintaining the chemistry of silicon nanoparticles. The success of these new drug delivery media would prevent the requirement of taking multiple medications a day and would provide another alternative for those who have dysphagia or prefer not to swallow medication.

Chapter 2 mainly discussed the synthesis of these biocompatible porous films using the NIPS and TIPS procedure. The NIPS procedure led to pores with the most uniform pore size, films that were not easily cracked, a consistency in morphology and pores of similar shape. Utilizing the TIPS procedure led to the formation of spherulites in many cases and films that were not durable so would easily crack when handled. The percentage of the polymer PCL in the di-solvent system DCM and DMSO that led to the pores that met the same parameters mentioned were also determined utilizing images of them from the SEM and the Feret's diameter of the pores. When loading the pSi particles in the films, physical entrapment was not the best method as pSi particles were randomly dispersed in the film but not necessarily in the depths of the pores. They were also not bound to the film and could easily be removed by spraying the films with nitrogen gas. Functionalizing the pSi particles with APTES and subsequently GTA as an effort to covalently bind them to the films was performed. However, the interactions between the primary amine and aldehyde were thought to be electrostatic. To form a covalent linkage, coupling agents such as DCC should be added in order to promote the formation of an amide. Ideally, this should be done to achieve the formation of a covalent bond between the pSi particles and the porous film. Many methods were used to determine the strength of the interaction between the pSi particles and the porous film and prevent the aggregation of pSi

particles. It was determined that dipping the films with the pSi particles in water and spraying the films with nitrogen gas as an effort to remove the loose pSi particles from the surface led to the best results. However, this would likely not work in a biological environment due to the presence of salt disrupting the electrostatic interactions between the pSi particles and the porous films so coupling agents should be used instead in order to form an amide between the APTES-functionalized pSi particles and PCL.

Chapter 3 encompassed loading CPT- a hydrophobic drug with fluorescent properties- into pSi particles then evaluating its release in an environment that resembled a biological one, such as water, and one that it is completely soluble in, such as DMSO. CPT was loaded in pSi using the submergence of pSi in a 0.1mg/mL solution of CPT in DMSO to achieve 1% w/w CPT loaded in pSi particles and 2% w/w CPT loaded in pSi particles- the volume of the solution was altered to achieve the different percentages. The release kinetics of the 1% w/w CPT loaded in pSi particles were evaluated in water to determine the trend of CPT release and the encapsulation efficiency was attempted to determine the amount of CPT that was released in the aqueous environment. It was determined that the number of pSi particles used needed to be very high or the amount of CPT needed to be increased as the release of the CPT was undetectable when determining the encapsulation efficiency. This is a reason that the loading percentage was increased and evaluated. PSi particles that were loaded 2% w/w CPT led to a similar trend when determining the release kinetics but led to samples with lower intensities. The amount of time pSi particles are likely submerged in the CPT/DMSO solution should be increased to maximize the amount of CPT loaded in the pSi particles. The encapsulation efficiency should also be evaluated of these particles, however, when evaluating it in water, the calibration curve of CPT in water should be redone as much of the CPT was not dissolved in the solution which led to similar intensities for different concentrations of CPT in water. I would suggest that the solutions are placed in the horn sonicator to mix the solution thoroughly before diluting the samples.

References

1. Prescription Drugs. (2019, February 13). Retrieved November 14, 2020, from https://hpi.georgetown.edu/rxdrugs/
2. Karki, S., Kim, H., Na, S., Shin, D., Jo, K., & Lee, J. (2016, June 06). Thin films as an emerging platform for drug delivery. Retrieved November 14, 2020, from https://www.sciencedirect.com/science/article/pii/S1818087616300368
3. Porous Silicon. (n.d.). Retrieved November 14, 2020, from https://www.sciencedirect.com/topics/pharmacology-toxicology-and-pharmaceutical-science/porous-silicon
4. Sailor, M. (2011, December 12). Porous Silicon in Practice: Preparation, Characterization and Applications. Retrieved November 14, 2020, from https://www.wiley.com/en-us/Porous Silicon in Practice: Preparation, Characterization and Applications-p-9783527313785
5. Reginald, E. (1997, December 1). Topoisomerase I Inhibitors. Retrieved November 16, 2020, from https://doi.org/10.1634/theoncologist.2-6-359
6. Gole, J. L., & Dixon, D. A. (1998). Transformation, Green to Orange-Red, of a Porous Silicon Photoluminescent Surface in Solution. *The Journal of Physical Chemistry B, 102*(1), 33-39. doi:10.1021/jp972214h
7. Korotcenkov, G. (2016). *Porous silicon: From formation to application*. Boca Raton: CRC Press, Taylor & Francis Group.
8. Tieu, T., Alba, M., Elnathan, R., Cifuentes-Rius, A., & Voelcker, N. H. (2019). Theranostics: Advances in Porous Silicon-Based Nanomaterials for Diagnostic and Therapeutic Applications (Adv. Therap. 1/2019). *Advanced Therapeutics, 2*(1), 1970001. doi:10.1002/adtp.201970001
9. Dongfei, L., Quan, P., & Salonen, J. (2018, June 14). Impact of Pore Size and Surface Chemistry of Porous Silicon Particles and Structure of Phospholipids on Their Interactions. Retrieved November 14, 2020, from https://pubs.acs.org/doi/10.1021/acsbiomaterials.8b00343
10. Schwartz MP, Cunin F, Cheung RW, Sailor MJ. Chemical modification of silicon surfaces for biological applications. Phys. Status Solidi A—Appl. Mat. 2005;202:1380–1384. [Google Scholar] [Ref list]
11. Xu, J. (2019). Preparation of Porous Silicon by Electrochemical Etching Methods and its Morphological and Optical Properties. *International Journal of Electrochemical Science*, 5188-5199. doi:10.20964/2019.06.10
12. Bodiford, N. K. (n.d.). *Fabrication of various designs of porous silicon-polymer composite scaffolds for drug delivery and tissue engineering applications* (Unpublished master's thesis). Texas Christian University.
13. Burham, N., Hamzah, A. A., & Majlis, B. Y. (2017). Self-Adjusting Electrochemical Etching Technique for Producing Nanoporous Silicon Membrane. *New Research on Silicon - Structure, Properties, Technology*. doi:10.5772/67719
14. Sun, J., & Almquist, B. (2018, November 4). Metal-Assisted Plasma Etching of Silicon: A Liquid-Free Alternative to MACE. Retrieved from https://chemrxiv.org/articles/preprint/Metal-Assisted_Plasma_Etching_of_Silicon_A_Liquid-Free_Alternative_to_MACE/6128237/1
15. Batchelor, L., Loni, A., Canham, L. T., Hasan, M., & Coffer, J. L. (2012). Manufacture of Mesoporous Silicon from Living Plants and Agricultural Waste: An Environmentally Friendly and Scalable Process. *Silicon, 4*(4), 259-266. doi:10.1007/s12633-012-9129-8
16. Botanicals, B. (n.d.). Bamboo Anatomy And Growth Habits. Retrieved November 29, 2020, from http://www.bamboobotanicals.ca/html/about-bamboo/bamboo-growth-habits.html

17. Kim, K. H., Lee, D. J., Cho, K. M., Kim, S. J., Park, J., & Jung, H. (2015). Complete magnesiothermic reduction reaction of vertically aligned mesoporous silica channels to form pure silicon nanoparticles. *Scientific Reports, 5*(1). doi:10.1038/srep09014
18. Tiwari, G., Tiwari, R., Sriwastawa, B., Bhati, L., Pandey, S., Pandey, P., & Bannerjee, S. (2012, January). Drug delivery systems: An updated review. Retrieved November 16, 2020, from https://www.ncbi.nlm.nih.gov/pmc/articles/PMC3465154/
19. Bhatia, S. (2016). Nanoparticles Types, Classification, Characterization, Fabrication Methods and Drug Delivery Applications. *Natural Polymer Drug Delivery Systems,* 33-93. doi:10.1007/978-3-319-41129-3_2
20. Anglin, E., Cheng, L., Freeman, W., & Sailor, M. (2008). Porous silicon in drug delivery devices and materials☆. *Advanced Drug Delivery Reviews, 60*(11), 1266-1277. doi:10.1016/j.addr.2008.03.017
21. Foraker AB, Walczak RJ, Cohen MH, Boiarski TA, Grove CF, Swaan PW. Microfabricated porous silicon particles enhance paracellular delivery of insulin across intestinal Caco-2 cell monolayers. Pharm. Res. 2003;20:110–116. [PubMed] [Google Scholar
22. Bayliss SC, Buckberry LD, Harris PJ, Tobin M. Nature of the silicon–animal cell interface. J. Porous Mater. 2000;7:191–195. [Google Scholar]
23. Boukherroub R, Wojtyk JTC, Wayner DDM, Lockwood DJ. Thermal hydrosilylation of undecylenic acid with porous silicon. J. Electrochem. Soc. 2002;149:59–63. [Google Scholar]
24. Digital microfluidics and delivery of molecular payloads with magnetic porous silicon chaperones. *Dorvee JR, Sailor MJ, Miskelly GM Dalton Trans. 2008 Feb 14; (6):721-30.*
25. Vasilev, K., Chen, H., & Murray, P. (2014). The Potential of Nanomaterials for Drug Delivery, Cell Tracking, and Regenerative Medicine 2013. *Journal of Nanomaterials, 2014,* 1-2. doi:10.1155/2014/872681
26. Kamaly, N., Yameen, B., Wu, J., & Farokhzad, O. C. (2016). Degradable Controlled-Release Polymers and Polymeric Nanoparticles: Mechanisms of Controlling Drug Release. *Chemical Reviews, 116*(4), 2602-2663. doi:10.1021/acs.chemrev.5b00346
27. Dhaliwal, K. (2018). Biodegradable Polymers and their Role in Drug Delivery Systems. *Biomedical Journal of Scientific & Technical Research, 11*(1). doi:10.26717/bjstr.2018.11.002056
28. Omidian, H., & Park, K. (2008). Swelling agents and devices in oral drug delivery. *Journal of Drug Delivery Science and Technology, 18*(2), 83-93. doi:10.1016/s1773-2247(08)50016-5
29. Saltzman, W. M. (2001). Controlled Drug Delivery Systems. *Drug Delivery*. doi:10.1093/oso/9780195085891.003.0015
30. Conoscenti, G., Carrubba, V. L., & Brucato, V. (2017). A Versatile Technique to Produce Porous Polymeric Scaffolds: The Thermally Induced Phase Separation (TIPS) Method. *Archives in Chemical Research, 01*(02). doi:10.21767/2572-4657.100012
31. Geetha, M. (2017). Polycaprolactone. *Comprehensive Medicinal Chemistry III*. doi:https://www.sciencedirect.com/topics/medicine-and-dentistry/polycaprolactone
32. Lee, S., Kang, J., & Kim, D. (2018). A Mini Review: Recent Advances in Surface Modification of Porous Silicon. *Materials, 11*(12), 2557. doi:10.3390/ma11122557
33. Cintil, J. (2004). Zeta Potential. Retrieved November 16, 2020, from https://www.sciencedirect.com/topics/materials-science/zeta-potential
34. U. (n.d.). Spherulites and optical properties. Retrieved November 22, 2020, from https://www.doitpoms.ac.uk/tlplib/polymers/spherulites.php
35. Reginald, E. (1997, December 1). Topoisomerase I Inhibitors. Retrieved November 16, 2020, from https://doi.org/10.1634/theoncologist.2-6-359